

Interface states and anomalous quantum oscillations in graphene hybrid structures

C. P. Puls,¹ N. E. Staley,¹ and Y. Liu^{1,*}

¹*Department of Physics, The Pennsylvania State University, University Park, PA 16802*

(Dated: June 4, 2022)

Abstract

One- and two-layer graphene have recently been shown to feature new physical phenomena such as unconventional quantum Hall effects [1, 2, 3] and prospects of supporting a non-silicon technological platform using epitaxial graphene [4, 5]. While both one- and two-layer graphene have been studied extensively, continuous sheets of graphene possessing both parts have not yet been explored. Here we report a study of such graphene hybrid structures. In a bulk hybrid featuring two large-area one- and two-layer graphene and an interface between them, two sets of Landau levels and features related to the interface were found. In edge hybrids featuring a large two-layer graphene with narrow one-layer graphene edges, we observed an anomalous suppression in quantum oscillation amplitude due to the locking of one- and two-layer graphene Fermi energies and emergent chiral interface states. These findings demonstrate the importance of these hybrid structures whose unique interface states and related phenomena deserve further studies.

Two novel unconventional integer quantum Hall effects (QHEs) have been discovered in one- and two-layer graphene [1, 2, 3]. The QHE in one-layer graphene (1LG) was shown to exist even up to room temperatures [6], not seen in any other material systems studied so far. The origin of the room-temperature QHE in 1LG is related to high mobility and large spacing between adjacent Landau levels, given by $E_{n_1} = v_F \sqrt{2e\hbar B n_1}$, where $v_F \approx 1 \times 10^6$ m/s is the Fermi velocity, e the electron charge, \hbar the Planck constant, B the magnetic field, and $n_1 = 0, 1, 2 \dots$ the Landau level index [1, 2]. For a two-layer graphene (2LG), $E_n = \hbar\omega_c \sqrt{n_2(n_2 - 1)}$, where $\omega_c = eB/m^*c$ is the cyclotron frequency, m^* the effective mass of charge carriers, c the speed of light, and $n_2 = 0, 1, 2 \dots$ again the index [3]. As a result, the spacing between Landau levels in 1LG can be many times larger than those of 2LG even in modestly large magnetic field. For example, setting $m^* = 0.08m_e$, a value consistent with experimental and theoretical values away from the charge neutral point [7], $E_{n_1} = (93 \text{ meV}) \sqrt{n_1}$ while $E_{n_2} = (12 \text{ meV}) \sqrt{n_2(n_2 - 1)}$ at $B = 8 \text{ T}$. Unlike a conventional two-dimensional electron gas (2DEG), both 1LG and 2LG possess a Landau level at zero energy. In charge biased 2LG, however, the degenerate zero-energy Landau level (corresponding to $n_2 = 0$ or 1) is split into two which are shifted to the top and the bottom of a bias-induced energy gap, removing degeneracy [7, 8]. A structure of a one- and two-layer graphene hybrid such as that shown in Fig. 1a allows one to probe for the first time a contiguous 2DEG featuring two sets of Landau levels of drastically different energy scales.

The possible existence of novel interface states presents another motivation for studying graphene hybrid structures. Edge states in uniform 1LG and 2LG have been the focus of much theoretical study recently [9]. However, the step edge formed at the boundary of the neighboring regions of a continuous graphene sheet with different thicknesses has received little attention. We are aware of only theoretical studies in which a semi-infinite 1LG was placed on top of an infinitely large 1LG. Charge redistribution [10] and enhanced local density of states at the step region [11] were revealed, but the interface states were not addressed explicitly. If one takes the perspective where a 1LG edge is fused to that of a 2LG, their respective edge states would have to be reorganized at the interface, particularly in a strong magnetic field when chiral edge states will most likely lead to behavior different from the edge states of either 1LG or 2LG.

Quantum oscillations were observed in a bulk hybrid structure (Fig. 1b and c) prepared by a lithography-free fabrication technique [12]. The hybrid was electron-doped initially,

most likely due to the diffusion of Au atoms into the gap region between the source and drain (see below). Large magnetoresistance ($\frac{\Delta R}{R}$) were found at all gate voltages (Fig. 2a). Previously, large magnetoresistance was found in pure 1LG [13]. Resistance oscillations due to the presence of Landau levels in both 1LG and 2LG were found in R vs. V_g (Fig. 2b). This can be made clear when the variation of the two-terminal conductance of the device, $\Delta\sigma$, obtained after subtracting a background is plotted as a function of V_g as shown in Fig. 2c for $B = 6$ T. The number of carriers any Landau level can accomodate is $\frac{fB}{\phi_0}$, where f is the Landau level degeneracy ($=4$ for both 1LG and 2LG), B is the applied magnetic field, and $\phi_0 = \frac{2\pi\hbar}{e}$ is the flux quantum. Thus we expect to see a V_g period of 8.3 V at $B = 6$ T, for example. Indeed, we see two sets of oscillations marked by red and blue dashed lines respectively (one with larger amplitude). The period is consistent with that expected for either 1LG or 2LG. Both sets of oscillations continue through the charge neutral point without a double period, which would be expected from a double-degenerate Landau level of unbiased 2LG. However, this is consistent with the lowest energy Landau levels in teh 2LG having been shifted to the bottom and the top of an energy gap (≈ 20 meV [7], see supplementary material) induced by a charge bias. Since the $n_1 = 0$ Landau level is located at zero carrier concentration and is half-degenerate for a fiven carrier type, the conductance peaks of the biased 2LG should be shifted from those of 1LG by hald the period, consistent with data shown in Fig. 2c. The observed small offset from the expected shift is due to a slight difference in doping. Unexpected additional conductance peaks were also found as indicated by black arrows in Fig. 2c, which we attribute to the interface states to be discussed below.

Edge hybrids featuring a large-area 2LG portion and narrow 1LG edges (Fig. 1c and d) showed different behavior. The flakes used, which were clearly 2LG based on our optical characterizations, were not imaged by AFM before the Au deposition because of the concern of possible damage of the flake by the AFM tip. However, the AFM imaging after the low temperature measurements were carried out suggest that 1LG strips of a width less than 200 nm were present at the edges of the bulk 2LG. These edge hybrids were found to exhibit a regular resistance oscillation (Fig. 3) due to the filling of Landau levels of the large 2LG portion.

It should be noted that in our hybrid devices, the resistance reaches a minimum in the R vs. V_g when the density of states (DOS) reaches a maximum as the Landau levels are filled.

In previous graphene studies, a longitudinal resistance maximum rather than a minimum is found when the Fermi energy is positioned at a Landau level in a standard Hall bar geometry [1, 2, 3] and a two-terminal device of a long 1LG stripe [14]. In both cases, the currents flow parallel to the graphene edges in most of the sample away from the electrodes. However, in our device configuration, the length of the graphene region between the source and drain is small compared to the width. The Hall voltage near the electrodes vanishes (shorted), thus the currents in our graphene device flow increasingly diagonally as the field increases. As a result, both longitudinal and transverse contributions in high magnetic fields lead to behavior different from those seen in conventional devices. This implies that in the bulk hybrid, the oscillations of the larger amplitude, including a resistance minimum found at the charge neutral point, correspond to the 1LG portion.

A dramatic suppression of the 2LG resistance oscillations over certain V_g ranges (Fig. 3a) was found in edge hybrids. The center of these V_g ranges over which the oscillations were suppressed (relative to the charge neutral point) varies roughly as \sqrt{jB} , where $j = 0, 1, 2, \dots$ is the index of the oscillation suppression and B is the magnetic field. Interestingly, the energy of Landau levels in 1LG and 2LG are $E_{n_1} \sim \sqrt{n_1 B}$ and $E_{n_2} \sim \sqrt{n_2(n_2 - 1)}$, where $n_{1,2} = 0, 1, 2, \dots$, respectively, as shown in Fig. 3c, which suggests that the suppression of the oscillations has its origin in the 1LG edges. To show this connection, we first note that $E_{n_2} \sim n_2$, where n_2 is sufficiently large. Given that each Landau level can hold an equal number of charge carriers, varying V_g , which increases the carrier density linearly, will change the Fermi energy, E_F , in 2LG linearly (Fig. 3c). So long as E_F of the 1LG is locked to that of 2LG in the edge hybrids, varying V_g is operationally equivalent to varying the energy. The observed suppression of 2LG resistance oscillations could then be seen as a resistance oscillation of 1LG superimposed on those of the 2LG.

To understand how the Fermi energy in the 1LG edges is locked to that of 2LG in edge hybrids we consider the very different energy scales for the Landau levels in the 1LG and 2LG. Using once more an effective charge carrier mass $m^* = 0.08 m_e$ in the 2LG, the Landau level spectrum for $B = 5$ T, for example, are shown in Fig. 4a for 1LG and charge biased 2LG (the breadths of the levels will be discussed below). As V_g is ramped up, charge carriers will first fill the lowest-energy Landau levels. The relatively large energy of the $n_1 = 1$ Landau level in 1LG would encourage electrons in the 1LG edges to fill the lower-energy Landau levels in 2LG after the $n_1 = 0$ level in 1LG is filled (Fig. 4a). This charge transfer between

the 1LG and 2LG will continue until the charge accumulation produces a sufficiently large electric field to counter further transfer. For example, at 5 T, the most charge transferred would be $\approx 5 \times 10^{12}$ electrons per cm^2 (the population of 10 Landau levels) when the Fermi energy is just below the $n_1 = 1$ Landau level. This mechanism locks the Fermi energy of the 1LG edges to that of the 2LG. In high magnetic fields, currents flow mostly on the edges (the interface region) of an edge hybrid. If its conductance variation can be made simply to be proportional to the total DOS, we can simulate the total sample conductance variation as a function of V_g (Fig. 4b). Comparing the simulated and experimental conductance variation shown in Fig. 4c, we find striking similarity between the two.

The details of the Landau levels and conductance spectra depend on several subtle factors. The conductance of 1LG (or 2LG) is increased when the Fermi energy enters the mobility edge near a Landau level. The size of the mobility edge, which is scaled with the Landau level broadening, is determined by disorder, which is expected to be larger in the 1LG edges than in 2LG bulk in our edge hybrids because the edges of each graphene sheet are not necessarily smooth and adsorbates tend to accumulate at the edges. Furthermore, inhomogeneity in charge transfer across the interface will also lead to corresponding variation in the gate voltage needed to place the Fermi energy at a Landau level. We have used a simple Gaussian peak to represent both of these complications in our simulation. As to the width of the charge transfer region, it should be on the order of charge screening length, suggested by theoretical studies to be on the order of 10-100 nm [15, 16], consistent with that estimated from the size of charge puddles in 1LG [14]. The exact length scale for our charge depletion region near the 1LG-2LG interface in the hybrid structures needs to be calculated theoretically and verified by future measurements.

Other unusual features seen in graphene hybrid structures may also be attributed to the presence of the interface. In the edge hybrids, as the Landau levels in the 2LG bulk and 1LG edges are matched, the quantum oscillation becomes less regular, with certain 2LG conductance peaks missing (Fig. 4c). In the bulk hybrid, small peaks were found in the conductance of the bulk hybrid that correspond to neither 1LG nor 2LG (see Fig. 2c). These additional peaks may be due to the interface region featuring energy states or Landau level filling rates different from that in the bulk because of charge transfer. The interface-related conductance peaks may even be significant enough to obscure the presence of a 2LG peak (between the middle two black arrows, Fig. 2c). However, the amplitudes of these

additional peaks are small, requiring further measurements to quantify. Finally, if charge transfer across the interface of charge neutral 1LG and 2LG occurs in zero field due to a work function difference between 1LG and 2LG, planar p-n junctions will then be expected. Pure 1LG p-n junctions produced by local gates have been shown to feature novel physical phenomena [17, 18, 19].

The presence of new interface states is expected to lead to other novel behavior in this unique graphene system where a 2DEG of Dirac fermions with a Berry phase of π meets with another unique 2DEG featuring a Berry phase of 2π and a tunable energy gap. In a magnetic field, the charge density is expected to vary spatially rapidly, resulting in a strong lateral electric field in the interface region, where the chiral edge states of 1LG and 2LG will meet. New interface states emerging from the coupling of these chiral states will have to be chiral as well, which should give rise to new interface phenomena. In addition, the charge transfer from 1LG to 2LG may distribute unequally on the upper and the lower sheets of the 2LG, which may modify the 2LG chiral edge states in the context of a bias induced gap. Finally, charge transfer is to be expected at step edges in epitaxial graphene where thickness varies even over a typical device length scale and will have implications for the performance of the device. All this makes graphene hybrid structures both an important graphene system to study and a technologically relevant issue to address in future research.

METHODS

Our graphene flakes were mechanically exfoliated from bulk graphite (The Asbury Graphite Mills, Inc., Asbury, NJ) and deposited onto an insulating substrate. The substrate was a chip cut from a heavily doped Si wafer topped with 300 nm of thermally grown SiO_2 . This allows the heavily doped Si to be used as a backgate through which we capacitively tune the number of charge carriers as well as the Fermi level in our devices. A change by 1 V in gate voltage, V_g , effectively adds 7×10^{10} electrons per cm^2 . Devices were fabricated using an all-dry, lithography-free method, employing a ultrathin quartz filament as a shadow mask [12, 20]. In the case of the bulk hybrid, the filament was placed across the interface between 1LG and 2LG (Figures 5a-b). The thickness of graphene flakes were determined by correlating optical characterization with AFM and Raman spectroscopy measurements.

ACKNOWLEDGMENTS

We would like to thank J. K. Jain, K. von Klitzing, J. Zhu, P. Lammert, and J. Banavar for useful discussions. This work was supported by DOE under Grant DE-FG02-04ER46159 and DOD ARO under Grant W911NF-07-1-0182.

* Electronic address: liu@phys.psu.edu

- [1] K. S. Novoselov, A. K. Geim, S. V. Morozov, D. Jiang, M. I. Katselson, I. V. Grigorieva, S. V. Dubonos, and A. A. Firsov, *Nature* **438**, 197 (2005).
- [2] Y. Zhang, Y.-W. Tan, L. Stormer, and P. Kim, *Nature* **438**, 201 (2005).
- [3] K. Novoselov, E. McCann, S. V. Morozov, V. I. Fal'ko, M. I. Katselson, U. Zeitler, D. Jiang, F. Schedin, and A. K. Geim, *Nature Physics* **2**, 177 (2006).
- [4] C. Berger, Z. Song, X. Li, X. Wu, N. Brown, C. Naud, D. Mayou, T. Li, J. Hass, A. N. Marchenkov, et al., *Science* **312**, 1191 (2006).
- [5] W. A. de Heer, C. Berger, X. Wu, P. N. First, E. H. Conrad, X. Li, T. Li, M. Sprinkle, J. Hass, M. L. Sadowski, et al., *Solid State Comm.* **143** (1-2), 92 (2007).
- [6] K. S. Novoselov, Z. Jiang, Y. Zhang, S. V. Morozov, H. L. Stormer, U. Zeitler, J. C. Maan, G. S. Boebinger, P. Kim, and A. K. Geim, *Science* **315**, 1379 (2007).
- [7] E. McCann, *Phys. Rev. B* **74** (2006).
- [8] E. V. Castro, K. S. Novoselov, S. V. Morozov, N. M. R. Peres, J. M. B. L. dos Santos, J. Nilsson, F. Guinea, A. K. Geim, and A. H. C. Neto, *Phys. Rev. Lett.* **99** (2007).
- [9] A. H. C. Neto, F. Guinea, N. M. R. Peres, K. S. Novoselov, and A. K. Geim, unpublished (arxiv:0709.1163v2 (2008)).
- [10] M. Arikawa, Y. Hatsugai, and H. Aoki, unpublished (arxiv:0805.3240) (2008).
- [11] E. V. Castro, N. M. R. Peres, J. M. B. L. dos Santos, A. H. C. Neto, and F. Guinea, unpublished (arxiv:0805.2161) (2008).
- [12] N. Staley, H. Wang, C. Puls, J. Forster, T. N. Jackson, K. McCarthy, B. Clouser, and Y. Liu, *Appl. Phys. Lett.* **90** (2006).
- [13] S. Cho and M. S. Fuhrer, *Phys. Rev. B* **77** (2008).
- [14] J. Martin, N. Akerman, G. Ulbricht, T. Lohmann, J. H. Smet, K. von Klitzing, and A. Yacoby,

- Nature **4**, 144 (2008).
- [15] B. Schklovskii, unpublished (arxiv:0706.4425) (2008).
 - [16] E. R. . S. D. Sarma, unpublished (arxiv:0803.0963) (2008).
 - [17] B. Huard, J. A. Sulpizio, N. Stander, K. Todd, B. Yang, and D. Goldhaber-Gordon, Phys. Rev. Lett. **98** (2007).
 - [18] J. R. Williams, L. DiCarlo, and C. M. Marcus, Science **317**, 638 (2007).
 - [19] D. A. Abanin and L. S. Levitov, Science **317**, 641 (2007).
 - [20] N. E. Staley, C. P. Puls, and Y. Liu, Phys. Rev. B **77** (2008).

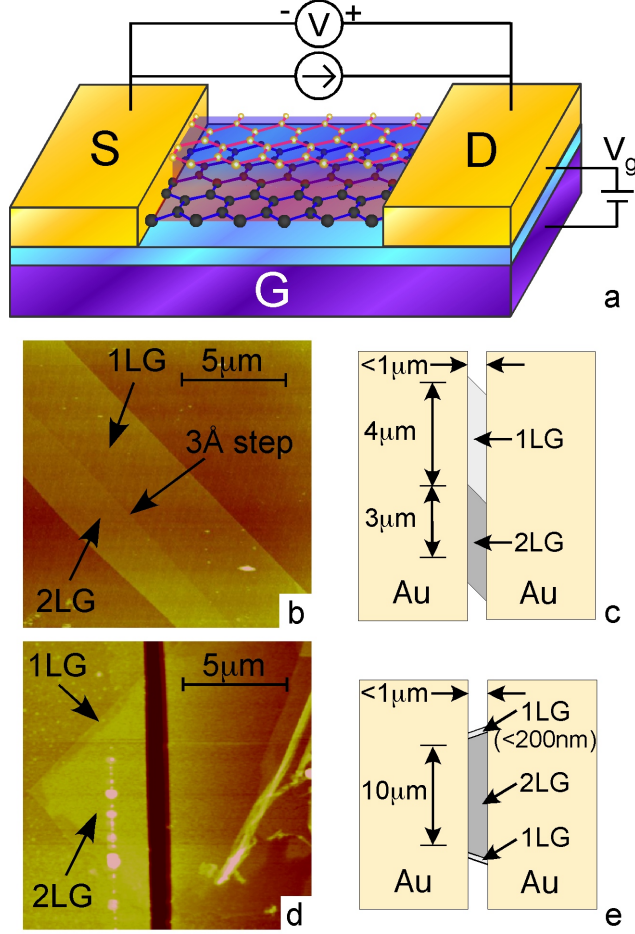


FIG. 1: a) Schematic of a hybrid field-effect structure prepared on a continuous graphene sheet with a 1LG and 2LG portion and a step edge. The source (S), drain (D), and gate (G) are indicated; b) Atomic force microscope (AFM) image of a bulk hybrid flake. A 3 Å step between large-area 1LG and 2LG portions is indicated; c) Dimensions of a bulk hybrid device prepared on the flake shown in (b); d) AFM image of an edge hybrid device with Au electrodes (taken after low-temperature measurements); e) Dimensions of the device shown in (d). The upper bound of the length of the graphene region between the electrodes is given by the filament size (around 1 μm for all samples). The actual length of the device can be as low as 40% of the filament size (see supplementary information).

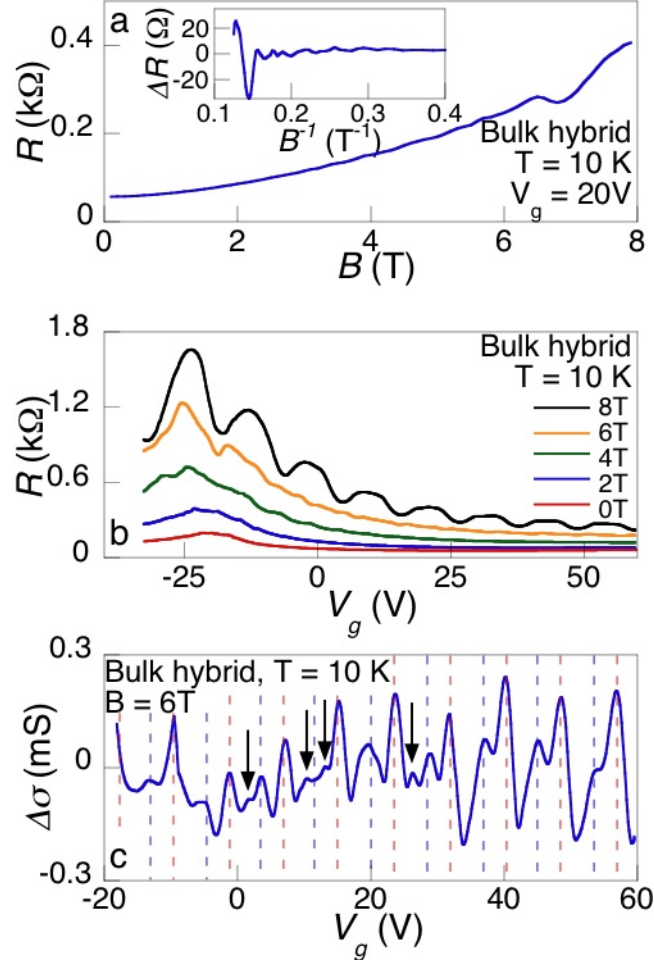


FIG. 2: a) Quantum oscillations seen in resistance (R) vs. magnetic field (B) at gate voltage $V_g = 20$ V. Inset: R vs. B^{-1} with a background removed; b) R vs. V_g in various B-fields as indicated; c) Conductance variation $\Delta\sigma$ vs. V_g at $B = 6$ T. The red and blue dashed lines indicate where the Fermi level sweeps through Landau levels in 1LG and 2LG, respectively. Black arrows point to unexpected peaks associated with the interface (see text).

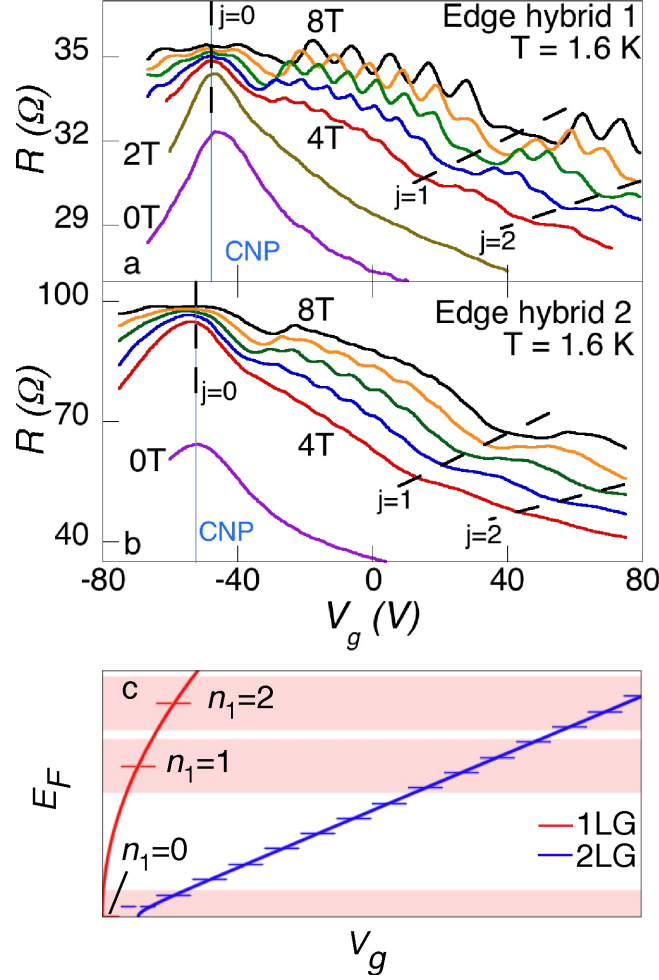


FIG. 3: Quantum oscillations in R vs. V_g of two devices prepared on edge hybrids at $B = 0, 2, 4, 5, 6, 7$, and 8 T (bottom) and $B = 0, 2, 4, 5, 6, 7$, and 8 T (top). Suppression of 2LG resistance oscillation peaks observed in field-dependent V_g ranges are indexed by j (see text). By analyzing the period of regular 2LG Shubnikov-de Haas oscillations in R vs. B^{-1} , we could determine the charge neutral points of the devices (see supplementary materials). A gap of ≈ 44 meV is expected in Edge hybrid 1, due to the charge doping [7], that splits the lowest energy Landau level in 2LG and places them at the top and bottom of the gap. The edge hybrids feature resistance maxima at the charge neutral point and at integer filling factors of multiples of four. Resistance minima correspond to peaks in the DOS; c) Theoretical E_F vs. V_g for 1LG and 2LG in a magnetic field. The horizontal ticks mark the Landau level energies of each system (the indices of 2LG Landau levels are not shown). The shaded areas represent the variation in E_F in 1LG edges due to factors described in text. Note that in 2LG, E_F is roughly linearly proportional to V_g .

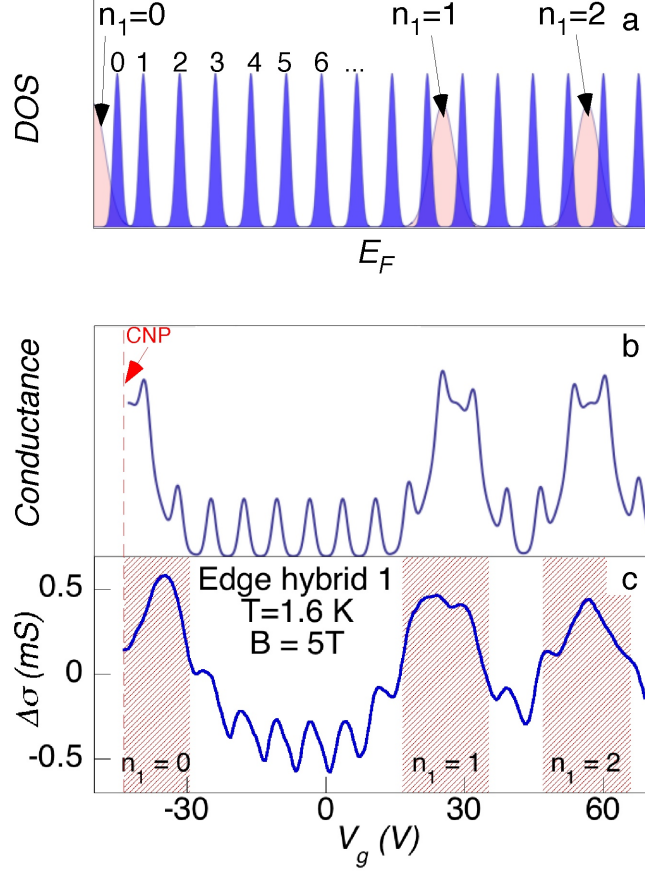


FIG. 4: a) Schematic of density of states *vs.* Fermi energy (E_F) showing Landau levels in 1LG and biased 2LG (see text); b) Simulated conductance variation *vs.* V_g as determined by total density of states, assuming that E_F of 1LG edges to that of 2LG; c) Experimental results of $\Delta\sigma$ *vs.* V_g for the edge hybrid device shown in the top of Fig. 4 for $B = 5$ T. The shaded areas show the ranges of conductance enhancements (resistance suppression) due to the presence of energy-matched 1LG Landau levels.